Glucosylation of catechol with the GTFA glucansucrase enzyme from Lactobacillus reuteri and sucrose as donor substrate

Te Poele, Evelien Maria; Grijpstra, Pieter; van Leeuwen, Sander S; Dijkhuizen, Lubbert

Published in:
BIOCONJUGATE CHEMISTRY

DOI:
10.1021/acs.bioconjchem.6b00018

Document Version
Publisher's PDF, also known as Version of record

Publication date:
2016

Bioconjugate Chemistry

Article

pubs.acs.org/bc

Glucosylation of Catechol with the GTFA Glucansucrase Enzyme from *Lactobacillus reuteri* and Sucrose as Donor Substrate

Evelien M. te Poele, Pieter Grijpstra, Sander S. van Leeuwen, and Lubbert Dijkhuizen*

Department of Microbiology, Groningen Biomolecular Sciences and Biotechnology Institute (GBB), University of Groningen, Nijenborgh 7, 9747 AG Groningen, The Netherlands

Supporting Information

ABSTRACT: Lactic acid bacteria use glucansucrase enzymes for synthesis of gluco-oligosaccharides and polysaccharides (α-glucans) from sucrose. Depending on the glucansucrase enzyme, specific α-glucosidic linkages are introduced. GTFA-ΔN (N-terminally truncated glucosyltransferase A) is a glucansucrase enzyme of *Lactobacillus reuteri* 121 that synthesizes the reuteran polysaccharide with (α1 → 4) and (α1 → 6) glycosidic linkages. Glucansucrases also catalyze glucosylation of various alternative acceptor substrates. At present it is unclear whether the linkage specificity of these enzymes is the same in oligo/polysaccharide synthesis and in glucosylation of alternative acceptor substrates. Our results show that GTFA-ΔN glucosylates catechol into products with up to at least 5 glucosyl units attached. These catechol glucosides were isolated and structurally characterized using 1D/2D ^{1}H NMR spectroscopy. They contained 1 to 5 glucose units with different (α1 → 4) and (α1 → 6) glycosidic linkage combinations. Interestingly, a branched catechol glucoside was also formed along with a catechol glucoside with 2 successive (α1 → 6) glycosidic linkages, products that are absent when only sucrose is used as both glycosyl donor and acceptor substrate.

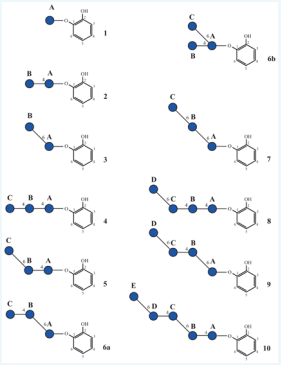

INTRODUCTION

Glucansucrases are extracellular enzymes with high molecular masses, most of them ranging 120−200 kDa. According to the carbohydrate-active enzymes (CAZy) classification system, they belong to the glycoside hydrolase family 70 (GH70)[1] and are only reported to occur in lactic acid bacteria, in members of the genera *Leuconostoc*, *Streptococcus*, *Lactobacillus*, and *Weissella*. As main activity they convert sucrose into α-glucan oligo- and polysaccharides. Glucansucrase enzymes strongly differ in reaction specificity, introducing one or more glycosidic linkage types [(α1 → 2), (α1 → 3), (α1 → 4), or (α1 → 6)] in their glucan products. Their polymers also differ in the degree and type of branching, and in molecular mass.[2−4]

GTFA-ΔN of *Lactobacillus reuteri* 121 produces a reuteran-type branched glucose polymer with both (α1 → 4) and (α1 → 6) glycosidic linkages.[5,6] Incubation of GTFA-ΔN with sucrose results in elongation of sucrose with glucose units via alternating (α1 → 4) and (α1 → 6) linkages into linear gluco-oligosaccharides up to a degree of polymerization (DP) of at least 12. Oligosaccharides with successive (α1 → 4) linkages were observed only up to DP4, but no linear (α1 → 6) structures were found. Simultaneously with oligosaccharide synthesis, also polymers were formed from the beginning of the reaction, suggesting that oligosaccharides longer than DP12 have higher affinity with the GTFA-ΔN enzyme and are rapidly elongated into branched reuteran with a high molecular mass (4×10^7 Da).[7,8]

Glucansucrases also glucosylate several other hydroxyl-group-containing molecules, in the so-called acceptor reaction.[2] Glycosylation is one of the most important reactions in nature and the glycosides formed often have improved physicochemical and biological properties, such as increased solubility, bioavailability, and stability.[9] Glycosylation may also improve bioactivity of antibiotics and modulate flavors and fragrances.[10] Glucansucrases are successfully used for glycosylation of acceptor substrates such as hydroquinone,[11] L-ascorbic acid,[12] and puerarin.[13]

Phenolic antioxidants like catechol are reported as inhibitors of proinflammatory pathways.[14−17] Zheng et al. (2008), for instance, have shown that catechol has anti-inflammatory and neuroprotective properties on cultured microglia. Microglia are the principle immune cells in the central nervous system; overactivation of microglia leads to the secretion of numerous proinflammatory mediators that cause neurotoxicity.[18,19] Catechols could therefore be considered as potential drug candidates for treating neurodegenerative diseases, such as Alzheimer's and Parkinson's disease, and other inflammatory disorders.[15] However, at physiological pH catechol easily auto-oxidizes, making it less suitable as a drug.[15] Glycosylation of catechol may result in more stable catechol glucosides with improved pharmacological and physicochemical properties. Glucosylation of catechol by a glucansucrase enzyme has been reported before;[20] however, no catechol-glucoside product characterization has been performed.

At present it is unknown whether glucansucrase enzymes glucosylate phenolic compounds with the same linkage

Received: January 10, 2016
Revised: February 16, 2016
Published: February 22, 2016

DOI: 10.1021/acs.bioconjchem.6b00018
Bioconjugate Chem. 2016, 27, 937−946

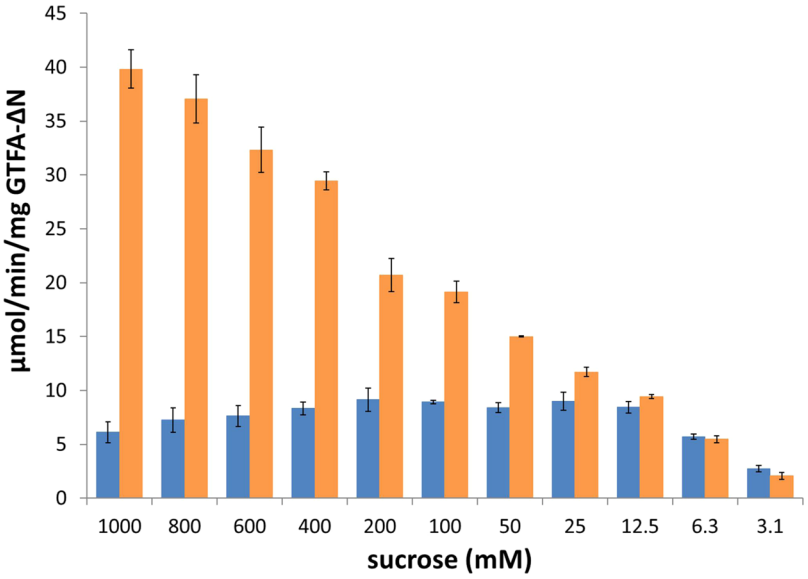

Figure 1. Transglycosylation (orange bars) and hydrolysis (blue bars) activity of GTFA-ΔN at different sucrose concentrations. The data represent the means of two independent enzyme activity assays.

specificity as used for oligo- and polysaccharide synthesis. In this study we used GTFA-ΔN to glucosylate catechol, and structurally characterized catechol glucoside products up to DP5 using 1D/2D ^{1}H NMR spectroscopy. Comparison of these catechol glucoside products with the oligosaccharides synthesized by GTFA-ΔN, when incubated with sucrose only, revealed not only interesting similarities, but also clear structural differences.

RESULTS

Synthesis of Catechol Glucosides Using the GTFA-ΔN Enzyme. GTFA-ΔN efficiently glucosylated catechol when incubated with 100 mM sucrose as the donor substrate. Sucrose was hydrolyzed as well, however, resulting in loss of glycosylation potential. To optimize the acceptor reaction for transglycosylation of catechol, the effect of sucrose concentration on the GTFA-ΔN transglycosylation to hydrolysis ratio was examined. For this, the transglycosylation and hydrolysis activities of GTFA-ΔN were determined in a range of 3.1−1000 mM sucrose (Figure 1). GTFA-ΔN showed higher transglycosylation to hydrolysis ratios with increasing sucrose concentrations, i.e., with a ratio of ∼0.76 at 3.1 mM sucrose, compared to ∼6.51 at 1000 mM sucrose. A higher overall transglycosylation activity also was observed with increasing sucrose concentrations. At 3.1 and 1000 mM sucrose the transglycosylation activity was 2.1 and 39.8 µmol/min/mg GTFA-ΔN, respectively, a ∼20-fold increase. For quantitative synthesis of catechol glucosides, 1000 mM sucrose was used as glucosyl donor.

Characterization of Catechol Glucosides Produced by GTFA-ΔN. A quantitative synthesis of catechol glucosides was performed by incubating 10 mL 250 mM catechol with three batches of 1000 mM of sucrose donor (added at t = 0, 45, and 90 min) to a total of 3000 mM sucrose, using 12.8 U (0.48 mg) GTFA-ΔN/mL. After prepurification on Strata-X SPE columns, catechol glucosides were isolated by preparative NP-HPLC (Figure 2), collecting 10 fractions. Relative abundances were determined based on NP-HPLC peak areas (Table 1).

Structural Analysis of Catechol Glucosides. NP-HPLC fractions were analyzed by high pH-anion exchange chromatography (HPAEC-PAD) (Supporting Information, Figure S1) and

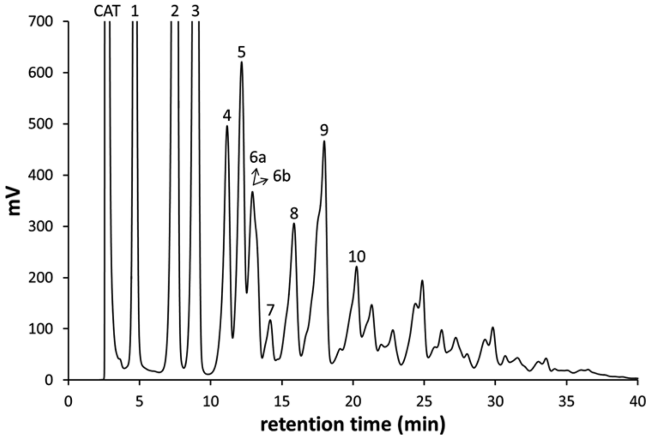

Figure 2. NP-HPLC profile of products of an incubation of 12.8 U (0.48 mg) GTFA-ΔN/mL with 250 mM catechol and 1000 mM sucrose for 135 min at 37 °C. At t = 45 and 90 min another 1000 mM sucrose was added to the incubation, resulting in a total amount of 3000 mM sucrose. The peak **1**−**10** compounds were isolated and structurally characterized.

Table 1. Compositions and Relative Abundance of NP-HPLC Fractions Determined by Peak Area and MALDI-TOF-MS

	m/z	composition	NP-HPLC area%
1	295.1	Hex_1Catechol	13.7
2	457.3	Hex_2Catechol	32.2
3	457.3	Hex_2Catechol	18.3
4	619.0	Hex_3Catechol	7.5
5	619.0	Hex_3Catechol	6.3
6	619.0	Hex_3Catechol	5.5
7	619.0	Hex_3Catechol	1.3
8	780.8	Hex_4Catechol	4.0
9	780.8	Hex_4Catechol	7.9
10	942.6	Hex_5Catechol	3.3

MALDI-TOF-MS (Table 1) to confirm purity and composition of the fractions. Analysis of fraction **6** on HPAEC-PAD (Supporting Information) showed one major and one medium peak, with a 2:1 ratio. MALDI-TOF-MS showed only one peak at

DOI: 10.1021/acs.bioconjchem.6b00018
Bioconjugate Chem. 2016, 27, 937−946

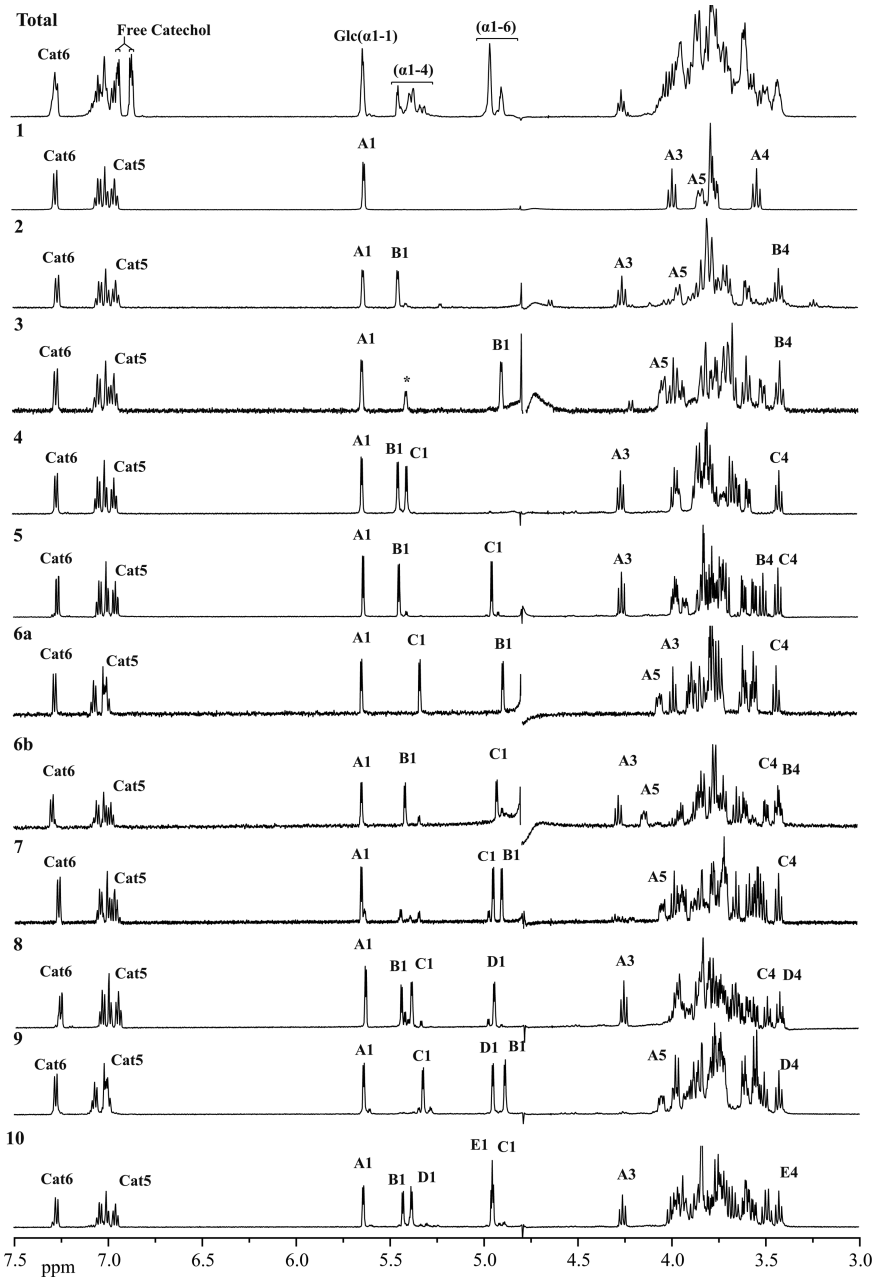

Figure 3. 1D ^{1}H NMR spectra of isolated structures **1**−**10** and the reaction mixture.

m/*z* 619.0, fitting with a Glc$_3$catechol structure. Fraction **6** was further separated on HPAEC-PAD under isocratic conditions with 150 mM NaOAc in 100 mM NaOH, resulting in fractions **6a** and **6b**.

Fraction 1. Using 1D (Figure 3) and 2D NMR (Supporting Information, Figure S2) spectroscopy all ^{1}H and ^{13}C chemical shifts could be determined (Table 2). Comparison of the catechol H-3, H-4, H-5, and H-6 values with those for free catechol revealed clear shifts, with the strongest shift in H-6 (from δ 6.937 to δ 7.266 ppm). The glucose H-1 signal is shifted significantly downfield to a unique position δ 5.626 ppm (Figure 3).[7,8,21] The $J_{1,2}$ coupling of 3.2 Hz indicates an α-linkage. Moreover, 2D ^{1}H−^{1}H ROESY spectra (not shown) revealed a cross-peak between **A-1** and **Cat-6**, indicating a glucosidic bond between Glc residue **A** and catechol. These data resulted in a structure α-D-Glc*p*-(1 → 1)-catechol, **A**1 → 1**Cat** for fraction **1** (Figure 4).

Fraction 2. The 1D ^{1}H NMR spectrum (Figure 3) showed α-anomeric peaks at δ 5.634 (**A** H-1; $J_{1,2}$ 3.2 Hz) and δ 5.449 (**B** H-1; $J_{1,2}$ 3.7 Hz), the former slightly shifted from the value observed for fraction **1**, and the latter fitting with values observed for α-D-Glc*p*-(1 → 4)- residues.[8,22] The catechol peaks showed a pattern fitting to a glucosylated structure. Using 2D NMR spectroscopy (Supporting Information, Figure S3) all ^{1}H and ^{13}C chemical shifts were assigned (Table 2). Residue **B** showed a ^{1}H and ^{13}C chemical shift pattern fitting a terminal residue. Particularly, the structural-reporter-group signal for terminal α-D-Glc*p*-residues of H-4 at δ 3.419 ppm supports this observation. Residue **A** shows significant downfield shifts in H-3 and H-4, to δ 4.255 ($\Delta\delta$ + 0.269) and δ 3.76 ($\Delta\delta$ + 0.224), respectively, compared to residue **A** in fraction **1**. These shifts fit with a 4-substitution of residue **A**.[22] This observation is further supported by the significant downfield shift of the C-4, to δ 77.4 ppm.[21] Moreover, ^{1}H−^{1}H ROESY spectroscopy (Supporting Information, Figure

DOI: 10.1021/acs.bioconjchem.6b00018
Bioconjugate Chem. 2016, 27, 937−946

Table 2. ^{1}H and ^{13}C Chemical Shift Values Determined for Catechol-Glucosides 1−10 by 1D and 2D NMR Spectroscopy[a]

	1		2		3		4		5		6a		6b	
residue	δ ^{1}H	δ ^{13}C	δ ^{1}H	δ ^{13}C	δ ^{1}H	δ ^{13}C	δ ^{1}H	δ ^{13}C	δ ^{1}H	δ ^{13}C	δ ^{1}H	δ ^{13}C	δ ^{1}H	δ ^{13}C
Cat 3	6.995	117.8	6.99	117.5	7.015	117.8	7.001	117.7	7.001	117.2	7.002	117.1	7.015	117.1
Cat 4	7.041	124.8	7.03	124.9	7.056	124.9	7.044	124.8	7.043	124.5	7.072	124.1	7.054	124.1
Cat 5	6.951	121.9	6.95	121.8	6.974	121.7	6.955	122.0	6.956	121.8	6.992	121.4	6.975	121.4
Cat 6	7.266	118.2	7.26	118.2	7.274	118.3	7.264	118.1	7.265	117.9	7.278	117.8	7.292	117.8
A 1	5.626 (3.2)	99.0	5.634 (3.2)	98.7	5.648 (3.4)	99.1	5.635 (3.2)	98.6	5.636 (3.1)	98.4	5.643 (3.1)	98.0	5.638 (3.2)	98.0
A 2	3.75	72.2	3.79	72.1	3.78	72.3	3.79	72.1	3.79	71.2	3.77	71.8	3.82	71.3
A 3	3.986	73.9	4.255	74.3	3.984	73.9	4.257	74.2	4.246	73.9	3.98	73.3	4.275	73.2
A 4	3.536	70.2	3.76	77.4	3.596	70.1	3.77	77.5	3.77	77.5	3.55	69.9	3.80	78.0
A 5	3.84	73.5	3.955	71.9	4.043	71.9	3.949	71.9	3.97	71.6	4.045	71.3	4.132	70.2
A 6a	3.81	61.2	3.81	61.1	3.70	66.4	3.80	61.2	3.81	61.0	3.76	66.2	3.84	66.8
A 6b	3.78	61.2	3.81		3.944		3.80		3.81		3.89		3.93	
B 1			5.449 (3.7)	100.4	4.901 (3.6)	98.5	5.444 (3.6)	100.4	5.445 (3.2)	100.4	4.888 (3.7)	97.9	5.406 (3.6)	99.8
B 2			3.587	72.4	3.508	72.4	3.64	72.5	3.608	72.3	3.55	71.3	3.59	72.1
B 3			3.694	73.9	3.668	73.9	3.970	74.2	3.71	73.6	3.87	73.6	3.70	73.2
B 4			3.419	70.1	3.419	70.4	3.65	77.5	3.506	70.0	3.61	78.1	3.410	69.7
B 5			3.73	73.6	3.72	72.9	3.83	72.0	3.920	71.9	3.80	70.6	3.70	72.1
B 6a			3.848	61.3	3.827	61.5	3.85	61.2	3.73	66.5	3.83	60.9	3.84	60.9
B 6b			3.76		3.76		3.80		3.98		3.77		3.75	
C 1							5.398 (3.6)	100.6	4.951 (3.1)	98.7	5.331 (3.7)	100.6	4.918 (3.7)	98.6
C 2							3.577	72.6	3.552	72.2	3.60	72.2	3.48	71.7
C 3							3.68	73.8	3.73	73.6	3.73	73.2	3.64	73.2
C 4							3.413	70.2	3.426	70.2	3.430	69.7	3.418	69.7
C 5							3.71	73.6	3.71	72.5	3.71	72.1	3.71	72.1
C 6a							3.84	61.2	3.84	61.2	3.84	60.9	3.84	60.9
C 6b							3.76		3.76		3.76		3.75	

	7		8		9		10	
residue	δ ^{1}H	δ ^{13}C	δ ^{1}H	δ ^{13}C	δ ^{1}H	δ ^{13}C	δ ^{1}H	δ ^{13}C
Cat 3	7.011	117.7	7.000	117.3	7.013	117.1	7.001	117.2
Cat 4	7.059	125.1	7.043	124.4	7.074	124.4	7.044	124.4
Cat 5	6.978	122.1	6.956	121.7	7.004	121.4	6.958	121.6
Cat 6	7.276	117.9	7.265	117.8	7.281	117.9	7.271	117.8
A 1	5.660 (3.5)	98.7	5.637 (3.4)	98.3	5.640 (3.5)	98.1	5.638 (3.4)	98.2
A 2	3.79	72.1	3.78	71.7	3.77	71.6	3.81	71.7
A 3	3.987	74.0	4.258	73.8	3.98	73.5	4.259	73.8
A 4	3.59	70.5	3.77	77.1	3.55	70.0	3.77	77.7
A 5	4.053	71.9	3.95	71.7	4.057	71.5	3.97	71.6
A 6a	3.73	66.5	3.82	60.8	3.78	66.4	3.80	61.0

DOI: 10.1021/acs.bioconjchem.6b00018
Bioconjugate Chem. 2016, 27, 937−946

Table 2. continued

	7		8		9		10	
residue	δ ^{1}H	δ ^{13}C	δ ^{1}H	δ ^{13}C	δ ^{1}H	δ ^{13}C	δ ^{1}H	δ ^{13}C
A 6b	3.95		3.82		3.89		3.80	
B 1	4.910 (3.7)	98.6	5.445 (3.5)	100.1	4.889 (3.7)	98.0	5.428 (3.7)	100.4
B 2	3.53	72.2	3.63	72.2	3.55	71.6	3.62	72.1
B 3	3.659	74.1	3.97	73.8	3.87	73.6	3.70	73.5
B 4	3.511	70.4	3.66	77.6	3.61	78.6	3.481	70.0
B 5	3.88	71.0	3.86	71.7	3.80	70.6	3.92	71.9
B 6a	3.72	66.2	3.89	61.0	3.86	60.8	3.77	66.8
B 6b	3.94		3.82		3.76		3.96	
C 1	4.957 (3.7)	98.6	5.390 (3.7)	100.2	5.326 (3.7)	100.7	4.948 (3.9)	98.4
C 2	3.552	72.4	3.59	72.3	3.61	72.1	3.61	71.7
C 3	3.72	73.9	3.68	73.5	3.74	73.4	4.004	73.8
C 4	3.429	70.4	3.48	70.0	3.51	69.6	3.65	77.9
C 5	3.70	72.6	3.91	71.8	3.92	71.6	3.86	70.7
C 6a	3.85	61.2	3.73	66.5	3.73	66.3	3.85	61.0
C 6b	3.76		3.97		3.97		3.76	
D 1			4.950 (3.4)	98.9	4.953 (3.2)	98.3	5.380 (3.4)	100.4
D 2			3.55	71.9	3.57	71.6	3.61	72.1
D 3			3.74	73.5	3.74	73.4	3.69	73.5
D 4			3.425	70.0	3.429	69.9	3.500	70.0
D 5			3.71	72.4	3.71	72.7	3.94	71.9
D 6a			3.85	61.0	3.85	60.8	3.74	66.4
D 6b			3.76		3.76		3.99	
E 1							4.956 (3.9)	98.4
E 2							3.57	71.7
E 3							3.74	73.5
E 4							3.426	70.0
E 5							3.71	72.3
E 6a							3.85	61.0
E 6b							3.76	

[a] ^{1}H chemical shifts derived directly from 1D ^{1}H NMR are shown in 3 decimals, shifts obtained from 2D spectra are shown with 2 decimal precision. For anomeric protons the $J_{1,2}$ coupling in Hz is shown between brackets.

DOI: 10.1021/acs.bioconjchem.6b00018
Bioconjugate Chem. 2016, 27, 937−946

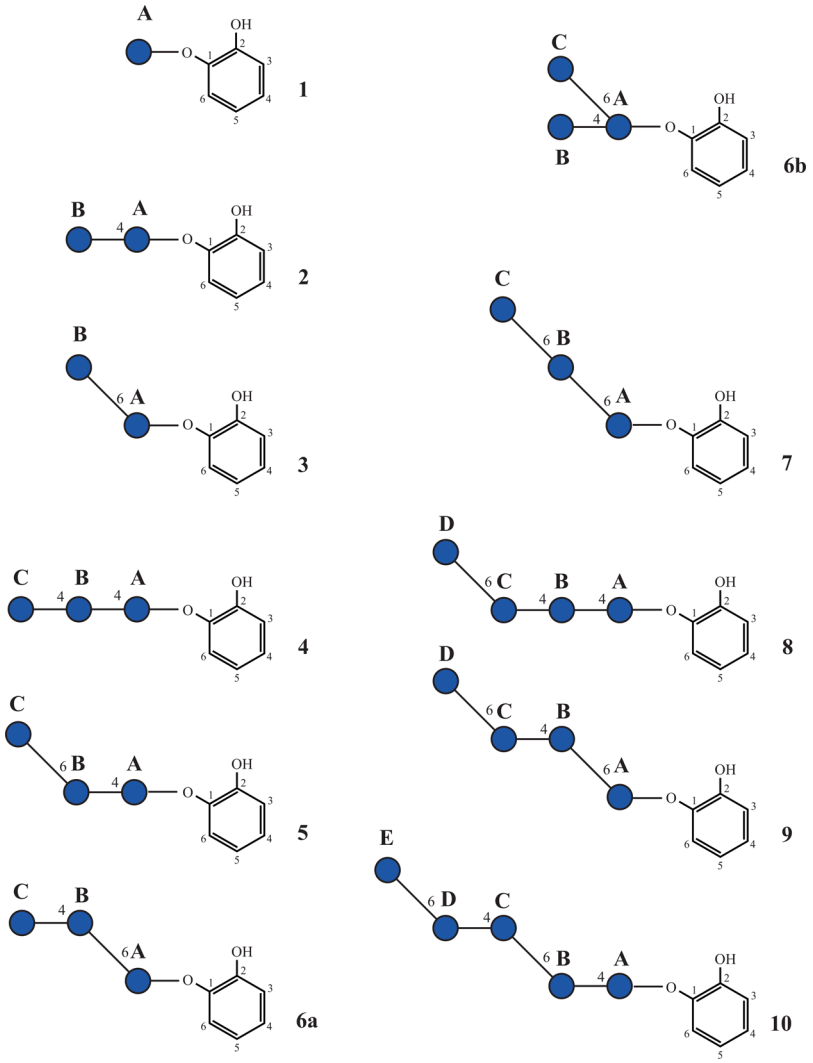

Figure 4. Established catechol glucoside structures obtained with 1D/2D ^{1}H and ^{13}C NMR spectroscopy. Glucose units are represented by blue circles.

S3) revealed inter-residual correlations between **B** H-1 and **A** H-4, and between **A** H-1 and **Cat** H-6. These data result in a structure for fraction **2** of α-D-Glc*p*-(1 → 4)-α-D-Glc*p*-(1 → 1)-catechol, i.e., **B**1 → 4**A**1 → 1**Cat** (Figure 4).

Fraction 3. The 1D ^{1}H NMR spectrum (Figure 3) showed major α-anomeric signals at δ 5.648 (**A** H-1; $J_{1,2}$ 3.4 Hz) and δ 4.901 (**B** H-1; $J_{1,2}$ 3.6 Hz). The minor peak at δ 5.447 most likely belongs to a contamination with fraction **2**. Using 2D NMR spectroscopy (Supporting Information, Figure S4) all ^{1}H and ^{13}C chemical shifts could be assigned (Table 2). The ^{1}H chemical shift pattern of residue **A** showed strong downfield shifts for H-5 and H-6b, whereas H-6a showed an upfield shift. These shifts fit with a 6-substitution of residue **A**.[22] Moreover, the C-6 signal was shifted downfield to 66.4 ppm, clearly indicating 6-substitution.[21] The pattern of ^{1}H and ^{13}C chemical shifts for residue **B** fit with those expected for a terminal α-D-Glc*p*-(1→6)-residue. Note in particular the H-4 at δ 3.419 and H-2 at 3.508 ppm.[8] ^{1}H−^{1}H ROESY spectroscopy (Supporting Information, Figure S4) revealed cross-peaks between **B** H-1 and **A** H-6a and between **A** H-1 and **Cat** H-6. These data lead to the conclusion that structure **3** is α-D-Glc*p*-(1→6)-α-D-Glc*p*-(1→1)-catechol, i.e., **B**1→6**A**1→1**Cat** (Figure 4).

Fraction 4. The 1D ^{1}H NMR spectrum (Figure 3) showed α-anomeric peaks at δ 5.635 (**A** H-1; $J_{1,2}$ 3.2 Hz), 5.444 (**B** H-1; $J_{1,2}$ 3.6 Hz) and 5.398 (**C** H-1; $J_{1,2}$ 3.6 Hz). 2D NMR spectroscopy (Supporting Information, Figure S5) was used to assign all ^{1}H and ^{13}C chemical shifts (Table 2). The chemical shift pattern of residue **A** fits with a 4-substituted Glc residue. Moreover, residue **B** shows shifts of H-3 and H-4 to δ 3.970 (Δδ + 0.276) and 3.65 (Δδ + 0.231), respectively, compared to residue **B** in structure **2**. These values, as well as the C-4 at 77.5 ppm, fit with a 4-substituted residue **B**. Residue **C** shows a chemical shift pattern fitting a terminal residue. ROESY spectroscopy showed interactions between **C** H-1 and **B** H-4, between **B** H-1 and **A** H-4, and between **A** H-1 and **Cat** H-6. These data result in a structure for **4** of α-D-Glc*p*-(1→4)-α-D-Glc*p*-(1→4)-α-D-Glc*p*-(1→1)-catechol, i.e., **C**1→4**B**1→4**A**1→1**Cat** (Figure 4).

Fraction 5. The 1D ^{1}H NMR spectrum showed α-anomeric signals at δ 5.636 (**A** H-1; $J_{1,2}$ 3.1 Hz), 5.445 (**B** H-1; $J_{1,2}$ 3.2 Hz), and 4.951 (**C** H-1; $J_{1,2}$ 3.1 Hz). Using 2D NMR spectroscopy (Supporting Information, Figure S6) all ^{1}H and ^{13}C chemical shift values were determined (Table 2). Residue **A** showed a pattern matching that of a 4-substituted residue (compare **A** in structures **2** and **4**), whereas residue **B** showed a pattern fitting a 6-substituted residue.[8,21,22] ROESY spectroscopy showed correlations between **C** H-1 and **B** H-6a and H-6b, between **B** H-1 and **A** H-4, and between **A** H-1 and **Cat** H-6. These data result in a structure for **5** consisting of α-D-Glc*p*-(1→6)-α-D-

DOI: 10.1021/acs.bioconjchem.6b00018
Bioconjugate Chem. 2016, 27, 937−946

Glc*p*-(1→4)-*α*-D-Glc*p*-(1→1)catechol, i.e., **C**1→6**B**1→4**A**1→1**Cat** (Figure 4).

Fraction 6a. Fraction **6a** showed a 1D ^{1}H NMR spectrum (Figure 3) with *α*-anomeric signals at *δ* 5.643 (**A** H-1; $J_{1,2}$ 3.1 Hz), 4.888 (**B** H-1; $J_{1,2}$ 3.7 Hz), 5.331 (**C** H-1; $J_{1,2}$ 3.7 Hz). 2D NMR spectroscopy (Supporting Information, Figure S7) revealed all ^{1}H and ^{13}C chemical shift values. The pattern of chemical shifts of residue **A** fit with a 6-substituted residue, similar to residue **A** in structure **3**, particularly notable are H-5, H-6a, and H-6b and C-6.[21,22] Residue **B** showed the pattern of a 4-substituted residue.[21,22] Residue **C** showed a pattern fitting with a terminal residue as shown by in an *α*-D-Glc*p*-(1→4)-configuration.[8,22] ROESY spectroscopy showed correlations between **C** H-1 and **B** H-4, between **B** H-1 and **A** H-6a and H-6b, and between **A** H-1 and **Cat** H-6. These data result in a structure for **6a** of *α*-D-Glc*p*-(1→4)-*α*-D-Glc*p*-(1→6)-*α*-D-Glc*p*-(1→1)-catechol, i.e., **C**1→4**B**1→6**A**1→1**Cat** (Figure 4).

Fraction 6b. The 1D ^{1}H NMR spectrum (Figure 3) of **6b** showed *α*-anomeric peaks at *δ* 5.638 (**A** H-1; $J_{1,2}$ 3.2 Hz), 5.406 (**B** H-1; $J_{1,2}$ 3.6 Hz), and 4.918 (**C** H-1; $J_{1,2}$ 3.7 Hz). Using 2D NMR spectroscopy (Supporting Information, Figure S8) all ^{1}H and ^{13}C chemical shifts were assigned (Table 2). Residue **A** showed a pattern in which H-3 (*δ* 4.275, Δ*δ* + 0.289), H-4 (*δ* 3.80; Δ*δ* + 0.264), H-5 (*δ* 4.132; Δ*δ* + 0.292), and H-6b (*δ* 3.93; Δ*δ* + 0.150) were shifted downfield, compared to residue **A** in structure **1**. Combined with ^{13}C chemical shifts for C-4 and C-6 at *δ* 78.0 and *δ* 66.8, respectively, these data indicate a 4,6-disubstituted Glc residue.[21,22] Residues **B** and **C** show a pattern fitting with a terminal residue, where **B** has an anomeric signal H-1 fitting with an (*α*1−4)-linkage, and residue **C** H-1 fitting with an (*α*1−6)-linkage. ROESY spectroscopy (Supporting Information, Figure S8) revealed correlations between **C** H-1 and **A** H-6a, between **B** H-1 and **A** H-4, and between **A** H-1 and **Cat** H-6. These data lead to the conclusion that structure **6b** is *α*-D-Glc*p*-(1→4)-[*α*-D-Glc*p*-(1→6)-]*α*-D-Glc*p*-(1→1)-catechol, i.e., **C**1→4[**B**1→6]**A**1→1**Cat** (Figure 4).

Fraction 7. The 1D ^{1}H NMR spectrum (Figure 3) showed *α*-anomeric peaks at *δ* 5.660 (**A** H-1; $J_{1,2}$ 3.5 Hz), 4.910 (**B** H-1; $J_{1,2}$ 3.7 Hz), and 4.957 (**C** H-1; $J_{1,2}$ 3.7 Hz). From 2D NMR spectroscopy (Supporting Information, Figure S9) all ^{1}H and ^{13}C chemical shifts could be assigned (Table 2). Residue **A** showed chemical shift patterns fitting a 6-substituted residue. Residue **B** showed a pattern corresponding with a 6-substituted *α*-D-Glc*p*-(1→6)-residue,[21,22] while residue **C** showed the pattern for a terminal residue in an *α*-D-Glc*p*-(1→6)- configuration. ROESY spectroscopy revealed cross-peaks between **C** H-1 and **B** H-6a, between **B** H-1 and **A** H-6a, and between **A** H-1 and **Cat** H-6. These data lead to a structure for 7 of *α*-D-Glc*p*-(1→6)-*α*-D-Glc*p*-(1→6)-*α*-D-Glc*p*-(1→1)-catechol, i.e., **C**1→6**B**1→6**A**1→1**Cat** (Figure 4).

Fraction 8. The 1D ^{1}H NMR spectrum (Figure 3) showed *α*-anomeric peaks at *δ* 5.637 (**A** H-1; $J_{1,2}$ 3.4 Hz), 5.445 (**B** H-1; $J_{1,2}$ 3.5 Hz), 5.390 (**C** H-1; $J_{1,2}$ 3.7 Hz), and 4.950 (**D** H-1; $J_{1,2}$ 3.4 Hz), fitting with two (*α*1→4)-linked and one (*α*1→6) linked glucose residue, beside one residue linking (*α*1→1) to catechol. Using 2D NMR spectroscopy (Supporting Information, Figure S10) all ^{1}H and ^{13}C chemical shifts were assigned (Table 2). The chemical shift patterns of residue **A** match that of residue **A** in structures, **2**, **4**, and **5**, suggesting 4-substitution. Residue **B** also showed chemical shift patterns fitting a 4-substituted residue; compare residue **B** in structure **4**. Residue **C** showed a pattern fitting 6-substitution.[21,22] Residue **D** showed a pattern fitting a terminal residue in an *α*-D-Glc*p*-(1→6)- configuration, as evidenced by the H-1 signal at *δ* 4.950. ROESY spectroscopy revealed correlations between **D** H-1 and **C** H-6a, between **C** H-1 and **B** H-4, between **B** H-1 and **A** H-4, and between **A** H-1 and **Cat** H-6. These data lead to a structure for **8** of *α*-D-Glc*p*-(1→6)-*α*-D-Glc*p*-(1→4)-*α*-D-Glc*p*-(1→4)-*α*-D-Glc*p*-(1→1)-catechol, i.e., **D**1→6**C**1→4**B**1→4**A**1→1**Cat** (Figure 4).

Fraction 9. The 1D ^{1}H NMR spectrum (Figure 3) showed *α*-anomeric signals at *δ* 5.640 (**A** H-1; $J_{1,2}$ 3.5 Hz), 4.889 (**B** H-1; $J_{1,2}$ 3.7 Hz), 5.326 (**C** H-1; $J_{1,2}$ 3.7 Hz), and 4.953 (**D** H-1; $J_{1,2}$ 3.2 Hz). These anomeric signals fit with a glucose linked to catechol, two (*α*1→6)-linked residues and one (*α*1→4)-linked residue. Using 2D NMR spectroscopy (Supporting Information, Figure S11) all ^{1}H and ^{13}C chemical shifts were assigned (Table 2). The chemical shift patterns show that residue **A** is 6-substituted, residue **B** is 4-substituted, residue **C** is 6-substituted, and residue **D** is terminal. ROESY spectroscopy showed cross-peaks between **D** H-1 and **C** H-6a, between **C** H-1 and **B** H-4, between **B** H-1 and **A** H-6a, and between **A** H-1 and **Cat** H-6. These data lead to a structure **9** of *α*-D-Glc*p*-(1→6)-*α*-D-Glc*p*-(1→4)-*α*-D-Glc*p*-(1→6)-*α*-D-Glc*p*-(1→1)-catechol, i.e., **D**1→6**C**1→4**B**1→6**A**1→1**Cat** (Figure 4).

Fraction 10. The 1D ^{1}H NMR spectrum (Figure 3) showed five *α*-anomeric signals at *δ* 5.638 (**A** H-1; $J_{1,2}$ 3.4 Hz), 5.428 (**B** H-1; $J_{1,2}$ 3.7 Hz), 4.948 (**C** H-1; $J_{1,2}$ 3.9 Hz), 5.380 (**D** H-1; $J_{1,2}$ 3.4 Hz), and 4.956 (**E** H-1; $J_{1,2}$ 3.9 Hz). These signals fit with one residue (**A**) linked to catechol, two (*α*1→6) linked residues, and two (*α*1→4)-linked residues. The H-4 peak at *δ* 4.259 indicates a 4-substitution of residue **A**, linked to catechol. Using 2D NMR spectroscopy (Supporting Information, Figure S12) all ^{1}H and ^{13}C chemical shifts were assigned (Table 2). The chemical shift patterns confirm a 4-substitution for residues **A** and **C**.[21,22] Both residues **B** and **D** show chemical shifts fitting a 6-substitution, as evidenced by C-6 at *δ* 66.8 and 66.4, respectively.[21] Residue **E** shows the pattern fitting a terminal residue. In the ROESY spectrum correlations are observed between **E** H-1 and **D** H-6a, between **D** H-1 and **C** H-4, between **C** H-1 and **B** H-6a, between **B** H-1 and **A** H-4, and between **A** H-1 and **Cat** H-6. These data lead to the proposed structure for **10**: *α*-D-Glc*p*-(1→6)-*α*-D-Glc*p*-(1→4)-*α*-D-Glc*p*-(1→6)-*α*-D-Glc*p*-(1→4)-*α*-D-Glc*p*-(1→1)-catechol, i.e., **E**1→6**D**1→4**C**1→6**B**1→4**A**1→1**Cat** (Figure 4).

Catechol Glycoside Mixture. 1D ^{1}H NMR spectroscopy (Figure 3) of the reaction mixture showed *α*-anomeric signals fitting with (*α*1→4)-linked (*δ* 5.33−5.46) and (*α*1→6)-linked (*δ* 4.48−4.96) residues in a relative abundance of 52% and 48%, respectively, indicating an almost equal amount of (*α*1→4)- and (*α*1→6)-linkages in the total product mixture.

DISCUSSION

The GTFA-ΔN enzyme is capable of efficiently glucosylating catechol (Structure **1**). The subsequent reactions also use **1** as an acceptor substrate, making diglucosylated catechol products with an (*α*1→4) (Structure **2**) and an (*α*1→6) linkage (Structure **3**). It should be noted that the main activity is (*α*1→4) elongation, with a ratio of structure **2**/**3** of 1.5, fitting the described activity and linkage specificity of the enzyme.[7,8] No structures were found with glucose moieties on both hydroxyl groups of the catechol molecule. The catechol will fit into the acceptor subsite to transfer glucose to one hydroxyl; however, the glucosyl-catechol substrate probably only fits in the acceptor subsite to allow transfer to the glucose moiety, and not to the second catechol hydroxyl.

DOI: 10.1021/acs.bioconjchem.6b00018
Bioconjugate Chem. 2016, 27, 937−946

Both diglucosylated structures are further elongated with (α1→4) and (α1→6) linkages. In the Glc_3catechol range five structures were isolated. Structures **4** and **5** are elongations of **2** with (α1→4) and (α1→6), respectively. Notably, the (α1→6) elongated peak has a higher surface-area than the (α1→4) elongation peak, indicating a slight preference for (α1→6) elongation. In a reaction with sucrose as both donor and acceptor substrate, the elongation with (α1→4) has a clear preference, while in a reaction with sucrose (donor) and maltose as acceptor substrate, the elongation with (α1→6) has almost exclusive priority.[7]

Elongation of **3** resulted in structures **6a** and **7**, with (α1→4) and (α1→6), respectively. The elongation with (α1→4) has preference here, while elongation with (α1→6) (Structure **7**) results in a minor peak. It should be noted, however, that the relative amount of this structural element is rather high, compared to the minimal amounts observed in incubations with maltose as acceptor substrate in previous studies.[7] Structure **6b** shows a branching element, which could be the result of either **2** or **3** receiving a branching moiety. The branching activity of GTFA-ΔN has been observed previously in incubations with maltose as acceptor substrate.[7,8] Structure **8** corresponds with a relatively large peak, stemming from (α1→6) elongation of **4**; the (α1→4) elongation product was not isolated, and could be in the further peaks after fraction **10**. Structure **9** occurs in similar quantities to structures **4** and **5** and corresponds with an (α1→6) elongation of **6a**. The structure for an (α1→4) elongation of **5** is missing, but probably corresponds with one of the minor peaks that were not isolated. Moreover, it should be noted that **10** is an (α1→6) elongation of this missing structure.

The catechol glucoside structures **5**, **6a**, **9**, and **10** fit very well with the described initial products formed by GTFA-ΔN when incubated with sucrose, where the main activity is that of an alternating (α1→4)/(α1→6) motif.[7] The relative intensities of the identified structures, however, seem to suggest a different preference for (α1→4) and (α1→6) elongation for catechol-glucosides than was previously observed for other donor/acceptor reactions.[7,8] This may be a result of the difference in the length of the glucoside acceptor, since on Glc_2catechol and Glc_3catechol there seems to be a preference for (α1→4) linkages, but in higher DP glucosides there is a more equal preference, due to the main activity forming alternating (α1→4)/(α1→6) sequences. Furthermore, two Glc_3catechol glucoside structures were identified that were not found in GTFA-ΔN incubations with only sucrose acting as both glucosyl donor and acceptor substrate,[7] i.e., a branched catechol glucoside with a →4,6-branch on the glucose attached to catechol (peak **6b**) and a product with two successive (α1→6) linked glucoses on α-D-Glc*p*-catechol (peak **7**). Similar structures were found when GTFA-ΔN was incubated with sucrose and maltose as acceptor substrate, i.e., → 4,6-branched glucose units on maltose and two successive (α1→ 6) linked glucoses attached to maltose.[7] This implies that catechol and maltose are bound differently than sucrose or a chain of growing glucan polymer in the acceptor site of GTFA-ΔN, leading to a different linkage pattern.

This report shows that the GTFA-ΔN enzyme of *L. reuteri* 121 glucosylated catechol into at least 11 different catechol glucoside products. These catechol glucosides may be more stable against auto-oxidation than free catechol at physiological pH and could therefore be suitable candidates for developing drugs for the treatment of neurodegenerative diseases and other inflammatory disorders. This could be tested by determining the anti-inflammatory and subsequent neuroprotective effects of the catechol glucosides on microglia and neuroblastoma cultured cells, as has been successfully shown for catechol and several catechol derivatives by Zheng et al.[15]

MATERIALS AND METHODS

Purification of Recombinant Glucansucrase Enzymes. Recombinant, N-terminally truncated GTFA-ΔN of *L. reuteri* 121[6,23] was produced as described by Meng et al.[24] and purified as described by Kralj et al.[6]

GTFA-ΔN Enzyme Activity Assays with Sucrose as Both Glucosyl Donor and Acceptor Substrate. Enzyme activity assays were performed with 11 different sucrose concentrations ranging from 3.1 to 1000 mM, in 25 mM sodium acetate (pH 4.7); 1 mM $CaCl_2$; and 3.2 U (0.12 mg)/mL GTFA-ΔN at 37 °C. To measure enzyme activities, samples of 100 μL were taken every 30 s over a period of 4 min and immediately inactivated with 20 μL 1000 mM NaOH for 30 min. The inactivated samples were diluted two times in deionized water, and from 10 μL of the diluted sample the glucose and fructose concentrations were determined enzymatically by monitoring the reduction of NADP with the hexokinase and glucose-6-phosphate dehydrogenase/phosphoglucose isomerase assay (Roche) as described previously.[25] Determination of the release of glucose and fructose from sucrose allowed calculation of the transglycosylation and hydrolytic activities of GTFA-ΔN.[26] The release of fructose corresponds to the total enzyme activity, the release of glucose to the hydrolytic activity, and the amount of fructose minus the amount of glucose corresponds to the transglycosylation activity. One unit (U) of enzyme is defined as the amount of enzyme required to produce 1 μmol monosaccharide per min in a reaction mixture containing 25 mM sodium acetate (pH 4.7); 1 mM $CaCl_2$; and 100 mM sucrose at 37 °C.

Quantitative Synthesis of Catechol Glucosides. For quantitative synthesis of catechol glucosides using GTFA-ΔN, a large scale enzymatic reaction was performed by incubating 10 mL 250 mM catechol with three batches of 1000 mM of sucrose donor (added at t = 0, 45, and 90 min) to a total of 3000 mM sucrose, using 12.8 U (0.48 mg) GTFA-ΔN/mL. Catechol glucosides were purified from the reaction mixture by solid phase extraction using Strata-X 33u Polymeric Reversed Phase columns (Phenomenex). Catechol glucosides were separated by semi preparative NP-HPLC and were collected manually. The solvent of the collected fractions was evaporated under a stream of nitrogen gas and the dried glucosides were dissolved in deionized water.

NP-HPLC. All HPLC analyses were performed on an UltiMate 3000 chromatography system (ThermoFischer Scientific, Amsterdam, The Netherlands), equipped with an Endurance autosampler (Spark Holland, The Netherlands). Catechol and catechol glucoside peaks were detected at 276 nm. In all cases a mobile phase of acetonitrile (solvent A) and 50 mM ammonium formate buffer, pH 4.4, (solvent B) was used.

For isolation of catechol glucosides, reaction products were separated on a Luna 10 μm NH_2 semipreparative chromatography column (250 mm × 10 mm, Phenomenex) and were manually collected at a flow-rate of 4.6 mL/min with a linear gradient of 80% to 55% solvent A over 40 min.

HPAEC-PAD. Purity of the collected catechol glucosides was analyzed with high-pH anion-exchange chromatography (HPAEC-PAD) on a CarboPac PA-1 column (250 mm × 4 mm, Dionex BV, Amsterdam, The Netherlands), using an ICS3000 Ion chromatograph (Dionex BV), equipped with a pulsed-amperometric detector (PAD) with a gold working

DOI: 10.1021/acs.bioconjchem.6b00018
Bioconjugate Chem. 2016, 27, 937−946

electrode (pulse potentials and durations: E1 + 0.1 V, 410 ms; E2 −2.0 V, 20 ms; E3 + 0.6 V, 10 ms, E4 −0.1 V, 60 ms), using a linear gradient of 30−300 mM sodium acetate in 100 mM NaOH (1 mL/min). Preparative separations were performed on a CarboPac PA-1 column (250 × 9 mm, Dionex BV, Amsterdam, The Netherlands) on an ICS5000 Ion chromatograph (ThermoFischer Scientific, Amsterdam, The Netherlands), eluted isocratically with 150 mM NaOAc in 100 mM NaOH (4 mL/min).

MALDI-TOF MS. Experiments were performed on an Axima mass spectrometer (Shimadzu Kratos Inc., Manchester, UK) equipped with a nitrogen laser (337 nm, 3 ns pulse width). Positive-ion mode spectra were recorded using the reflector mode at a resolution of at least 5000 full width at half maximum (fwhm) and acquired with software-controlled pulse-delayed-extraction optimized for m/z 1500. Mass spectra were recorded from 1 to 5000 Da, with ion-gate blanking set to 200 Da. Samples were prepared by mixing 1 μL purified glucoside with 1 μL 10 mg/mL 2,5-dihydroxybenzoic acid in 70% ACN as matrix solution.

NMR Spectroscopy. One-dimensional ^{1}H NMR, 2D ^{1}H−^{1}H, and 2D ^{13}C−^{1}H correlation spectra were recorded at a probe temperature of 298 K on a Varian Inova 600 spectrometer (NMR Department, University of Groningen). Samples were exchanged twice with 99.9 atom % D_2O (Cambridge Isotope Laboratories Ltd., Andover, MA) with intermediate lyophilization, finally dissolved in 650 μL D_2O. ^{1}H and ^{13}C chemical shifts are expressed in ppm in reference to internal acetone (δ ^{1}H 2.225; δ ^{13}C 31.08). 1D 600-MHz ^{1}H NMR spectra were recorded with 5000 Hz spectral width at 16k complex data points, using a WET1D pulse to suppress the HOD signal. 2D ^{1}H−^{1}H COSY spectra were recorded in 256 increments in 4000 complex data points with a spectral width of 5000 Hz. 2D ^{1}H−^{1}H TOCSY spectra were recorded with MLEV17 mixing sequences with 30, 50, and 150 ms spin-lock times. 2D ^{13}C−^{1}H HSQC spectra were recorded with a spectral width of 5000 Hz in t_2 and 10 000 Hz in t_1 direction. 2D ^{1}H−^{1}H ROESY spectra with a mixing time of 300 ms were recorded in 128 increments of 4000 complex data points with a spectral width of 5000 Hz. All spectra were processed using MestReNova 5.3 (Mestrelabs Research SL, Santiago de Compostella, Spain), using Whittaker Smoother baseline correction.

■ ASSOCIATED CONTENT

Supporting Information

The Supporting Information is available free of charge on the ACS Publications website at DOI: 10.1021/acs.bioconjchem.6b00018.

HPAEC-PAD profiles of the total reaction mixture and fractions **1**−**10**; relevant parts of the 1D ^{1}H NMR, ^{1}H−^{1}H COSY, TOCSY (150 ms mixing time), ROESY, and ^{13}C−^{1}H HSQC spectra of fractions **1**−**10** (PDF)

■ AUTHOR INFORMATION

Corresponding Author

*Tel: +31503632150; Fax: +31503632154; E-mail: L.Dijkhuizen@rug.nl.

Notes

The authors declare no competing financial interest.

■ ACKNOWLEDGMENTS

We thank Geralt ten Kate for HPAEC-PAD analysis. EtP and LD acknowledge financial support through the EU FP7-project "Novosides" (grant agreement nr. KBBE-4-265854). P.G. and S.v.L. acknowledge financial support from the University of Groningen.

■ REFERENCES

(1) Lombard, V., Golaconda Ramulu, H., Drula, E., Coutinho, P. M., and Henrissat, B. (2014) The carbohydrate-active enzymes database (CAZy) in 2013. *Nucleic Acids Res. 42*, D490−D495.

(2) Leemhuis, H., Pijning, T., Dobruchowska, J. M., van Leeuwen, S. S., Kralj, S., Dijkstra, B. W., and Dijkhuizen, L. (2013) Glucansucrases: three-dimensional structures, reactions, mechanism, α-glucan analysis and their implications in biotechnology and food applications. *J. Biotechnol. 163*, 250−272.

(3) Monchois, V., Willemot, R.-M., and Monsan, P. (1999) Glucansucrases: mechanism of action and structure-function relationships. *FEMS Microbiol. Rev. 23*, 131−151.

(4) Monsan, P., Remaud-Siméon, M., and André, I. (2010) Transglucosidases as efficient tools for oligosaccharide and glucoconjugate synthesis. *Curr. Opin. Microbiol. 13*, 293−300.

(5) Kralj, S., van Geel-Schutten, G. H., Rahaoui, H., Leer, R. J., Faber, E. J., van der Maarel, M. J. E. C., and Dijkhuizen, L. (2002) Molecular characterization of a novel glucosyltransferase from *Lactobacillus reuteri* strain 121 synthesizing a unique, highly branched glucan with α-(1−4) and α(1−6) glucosidic bonds. *Appl. Environ. Microbiol. 68*, 4283−4291.

(6) Kralj, S., van Geel-Schutten, G. H., van der Maarel, M. J. E. C., and Dijkhuizen, L. (2004) Biochemical and molecular characterization of *Lactobacillus reuteri* 121 reuteransucrase. *Microbiology 150*, 2099−2112.

(7) Dobruchowska, J. M., Meng, X., Leemhuis, H., Gerwig, G. J., Dijkhuizen, L., and Kamerling, J. P. (2013) Gluco-oligomers initially formed by the reuteransucrase enzyme of *Lactobacillus reuteri* 121 incubated with sucrose and malto-oligosaccharides. *Glycobiology 23*, 1084−1096.

(8) van Leeuwen, S. S., Kralj, S., van Geel-Schutten, I. H., Gerwig, G. J., Dijkhuizen, L., and Kamerling, J. P. (2008) Structural analysis of the α-D-glucan (EPS35−5) produced by the *Lactobacillus reuteri* strain 35−5 glucansucrase GTFA enzyme. *Carbohydr. Res. 343*, 1251−1265.

(9) Davies, G. J. (2001) Sweet secrets of synthesis. *Nat. Struct. Biol. 8*, 98−100.

(10) Desmet, T., Soetaert, W., Bojarová, P., Křen, V., Dijkhuizen, L., Eastwick-Field, V., and Schiller, A. (2012) Enzymatic glycosylation of small molecules: challenging substrates require tailored catalysts. *Chem. - Eur. J. 18*, 10786−10801.

(11) Seo, E.-S., Kang, J., Lee, J.-H., Kim, G.-E., Kim, G. J., and Kim, D. (2009) Synthesis and characterization of hydroquinone glucoside using *Leuconostoc mesenteroides* dextransucrase. *Enzyme Microb. Technol. 45*, 355−360.

(12) Kim, Y.-M., Yeon, M. J., Choi, N.-S., Chang, Y.-H., Jung, M. Y., Song, J. J., and Kim, J. S. (2010) Purification and characterization of a novel glucansucrase from *Leuconostoc lactis* EG001. *Microbiol. Res. 165*, 384−391.

(13) Ryu, Y. B., Park, T., Jeong, H. J., Kim, J., Park, S., Kim, J., Kim, D., Kim, Y., and Lee, W. S. (2012) Enzymatic synthesis of puerarin glucosides using *Leuconostoc dextransucrase*. *J. Microbiol. Biotechnol. 22*, 1224−1229.

(14) Ma, Q., and Kinneer, K. (2002) Chemoprotection by phenolic antioxidants. Inhibition of tumor necrosis factor alpha induction in macrophages. *J. Biol. Chem. 277*, 2477−2484.

(15) Zheng, L. T., Ryu, G.-M., Kwon, B.-M., Lee, W.-H., and Suk, K. (2008) Anti-inflammatory effects of catechols in lipopolysaccharide-stimulated microglia cells: inhibition of microglial neurotoxicity. *Eur. J. Pharmacol. 588*, 106−113.

(16) Knuth, S., Schübel, H., Hellemann, M., and Jürgenliemk, G. (2011) Catechol, a bioactive degradation product of salicortin, reduces TNF-α induced ICAM-1 expression in human endothelial cells. *Planta Med. 77*, 1024−1026.

DOI: 10.1021/acs.bioconjchem.6b00018
Bioconjugate Chem. 2016, 27, 937−946

(17) Dileep, K. V., Tintu, I., Mandal, P. K., Karthe, P., Haridas, M., and Sadasivan, C. (2012) Binding to PLA2 may contribute to the anti-inflammatory activity of catechol. *Chem. Biol. Drug Des. 79*, 143−147.
(18) González-Scarano, F., and Baltuch, G. (1999) Microglia as mediators of inflammatory and degenerative diseases. *Annu. Rev. Neurosci. 22*, 219−240.
(19) Block, M. L., Zecca, L., and Hong, J.-S. (2007) Microglia-mediated neurotoxicity: uncovering the molecular mechanisms. *Nat. Rev. Neurosci. 8*, 57−69.
(20) Meulenbeld, G. H., and Hartmans, S. (2000) Transglycosylation by *Streptococcus mutans* GS-5 glucosyltransferase-D: acceptor specificity and engineering of reaction conditions. *Biotechnol. Bioeng. 70*, 363−369.
(21) Bock, K., and Pedersen, C. (1983) Carbon-13 Nuclear Magnetic Resonance Spectroscopy of Monosaccharides. *Adv. Carbohydr. Chem. Biochem. 41*, 27−66.
(22) van Leeuwen, S. S., Leeflang, B. R., Gerwig, G. J., and Kamerling, J. P. (2008) Development of a 1H NMR structural-reporter-group concept for the primary structural characterisation of α-D-glucans. *Carbohydr. Res. 343*, 1114−1119.
(23) Kralj, S., van Geel-Schutten, G. H., Dondorff, M. M. G., Kirsanovs, S., van der Maarel, M. J. E. C., and Dijkhuizen, L. (2004) Glucan synthesis in the genus *Lactobacillus*: isolation and characterization of glucansucrase genes, enzymes and glucan products from six different strains. *Microbiology 150*, 3681−3690.
(24) Meng, X., Dobruchowska, J. M., Pijning, T., López, C. A., Kamerling, J. P., and Dijkhuizen, L. (2014) Residue Leu940 has a crucial role in the linkage and reaction specificity of the glucansucrase GTF180 of the probiotic bacterium *Lactobacillus reuteri* 180. *J. Biol. Chem. 289*, 32773−32782.
(25) Mayer, R. M. (1987) Dextransucrase: a glucosyltransferase from *Streptococcus sanguis*. *Methods Enzymol. 138*, 649−661.
(26) van Geel-Schutten, G. H., Faber, E. J., Smit, E., Bonting, K., Smith, M. R., Ten Brink, B., Kamerling, J. P., Vliegenthart, J. F. G., and Dijkhuizen, L. (1999) Biochemical and structural characterization of the glucan and fructan exopolysaccharides synthesized by the *Lactobacillus reuteri* wild-type strain and by mutant strains. *Appl. Environ. Microbiol. 65*, 3008−3014.

DOI: 10.1021/acs.bioconjchem.6b00018
Bioconjugate Chem. 2016, 27, 937−946